Sulfur Dioxide in the Atmosphere of Venus
I. Sounding Rocket Observations

William E. McClintock, Charles A. Barth, and Richard A. Kohnert

Laboratory for Atmospheric and Space Physics
University of Colorado, Boulder
1234 Innovation Drive
Boulder, Co 80303-7814
Ph: 303-492-8407 Fax: 303-492-6444
E-mail: mcclint@pisces.colorado.edu

15 Pages
6 Figures
3 Tables

Keywords: Atmospheres, Composition
Spectroscopy
Ultraviolet Observations
Venus

Rocket Observations of SO_2 in the Atmosphere of Venus

William E. McClintock
Laboratory for Atmospheric and Space Physics
University of Colorado, Boulder
1234 Innovation Drive
Boulder, Co 80303-7814
Ph: 303-492-8407 Fax: 303-492-6444
E-mail: mcclint@pisces.colorado.edu

Abstract

In this paper we present ultraviolet reflectance spectra obtained during two sounding rocket observations of Venus made during September 1988 and March 1991. We describe the sensitivity of the derived reflectance to instrument calibration and show that significant artifacts can appear in that spectrum as a result of using separate instruments to observe both the planetary radiance and the solar irradiance.

We show that sulfur dioxide is the primary spectral absorber in the 190 - 230 nm region and that the range of altitudes probed by these wavelengths is very sensitive to incidence and emission angles. In a following paper Na *et. al.* (1994) show that sulfur monoxide features are also present in these data. Accurate identification and measurement of additional species require observations in which both the planetary radiance and the solar irradiance are measured with the same instrument.

The instrument used for these observations is uniquely suited for obtaining large phase angle coverage and for studying transient atmospheric events on Venus because it can observe targets within 18° of the sun while earth orbiting instruments are restricted to solar elongation angles $\geq 45°$.

Introduction

Barker (1979) reported the first detection of sulfur dioxide in the atmosphere of Venus. He used a ground based high resolution spectrograph to observe absorption bands near 300 nm in the near ultraviolet reflection spectrum of the planet. Since its discovery, SO_2 has been extensively observed in the middle ultraviolet near 205 nm. Stewart *et al.* (1979) identified SO_2 as the species responsible for absorption features observed in a 1.3 nm resolution reflection spectrum using the Pioneer Venus Orbiter Ultraviolet Spectrometer (PVOUVS). Conway *et al.* (1979) confirmed this identification using a 0.1 nm resolution spectrum of Venus obtained with the International Ultraviolet Explorer (IUE). They showed that absorption bands observed in the region 208-218 nm closely match high resolution laboratory spectra of SO_2. Na *et al.* (1990) have used 200 - 218 nm IUE spectra taken in 1979 and 1987 to model the distribution of SO_2 above the cloud tops.

In this paper we present ultraviolet reflectance spectra obtained during two sounding rocket observations of Venus made during September 1988 and March 1991. We show that SO_2 is the primary spectral absorber in the 190 - 230 nm region and that the range of altitudes probed by these wavelengths is very sensitive to incidence and emission angles. Na *et. al.* (1990) have identified absorption bands due to SO in their IUE data and have used them to model the vertical distribution of SO above the cloud tops. We show that detection of additional species which absorb in this wavelength range will be most accurately accomplished using an instrument which can view both the planetary radiance and the solar irradiance.

In a following paper Na *et. al.* (1994) use the observations reported here to refine their determination of SO and to derive the spatial distribution of SO_2 above the cloud tops in 1988. They compare these results with PVOUVS, IUE, and Venera-15 (Zasova *et. al.* 1993) observations of SO_2.

Instrument Description

The rocket instrument consists of a Cassegrain style telescope and an Ebert - Fastie spectrometer coupled to a photon counting microchannel plate detector using CODACON (CODed Anode CONverter) readout electronics. Table I summarizes the instrument parameters. McClintock *et al.* (1982) described the design and performance of an early version of this instrument.

Here we summarize modifications which we have made in order to obtain spatially resolved spectra of Venus in the wavelength range 190 - 230 nm.

Telescope

The original telescope relied on the rocket attitude control system (ACS) for absolute pointing accuracy and stability. Offsets between the telescope optic axis and the star tracker limited the absolute pointing accuracy of the telescope to 2 arc minutes. Image jitter in the focal plane of the telescope was typically 20 arc seconds. The spectrograph used a square aperture with a 6 arc minute square field of view to capture the entire image of the planet.

In 1984 we installed a spectrograph slit jaw camera and an internal Image Motion Stabilization System (IMSS) in the telescope in order to achieve high pointing accuracy and stability. The IMSS is composed of an articulated secondary mirror and an optical error sensor used in a feedback loop. The secondary mirror is mounted on the shaft of a balanced gimbal assembly which allows it to pivot about a point behind its vertex. An optical sensor located near the focal plane of the telescope provides feedback for mirror control. Approximately 10 percent of the planet signal is directed toward a quadrant anode silicon photodiode by a beam splitter. Amplified error signals produced by the diode drive brushless torque motors which position the secondary mirror to stabilize the image of the planet in the telescope focal plane. During flight we can monitor and adjust the absolute position of the planet in the telescope focal plane to sub arc second accuracy using the spectrograph slit jaw camera and ground commands sent to the IMSS.

We also modified the optical figure of the original telescope mirrors from a Cassegrain design (parabolic primary mirror - hyperbolic secondary mirror) to a tilted aplanat design (both mirrors hyperbolic) so that targets located at off axis field positions can be repositioned to the center without degrading image quality (Bottema and Woodruff, 1971). Laboratory tests demonstrated that for a 0.5 arc second diameter source located up to 3 arc minutes off the optic axis, the telescope produces centered images which have full width half maxima less than 1.5 arc seconds.

Spectrograph and Detector

For the 1988 flight we replaced the spectrograph entrance aperture with a 0.01 x 1.59 mm slit resulting in a 0.9x 137 arc second field of view. The original spectrograph used a fixed grating mount and a grating with a ruling density of 2400 g/mm. It imaged the spectrum onto a 1 x 1024 CODACON detector with 0.025 mm pixel spacing. This configuration provided a spectral coverage of approximately 38.5 nm and a spectral resolution 0.2 nm. After the 1988 flight we installed a grating drive in the spectrograph which allows us to cover the wavelength range 190 -328 nm with 4 grating steps.

Sunshade and Telescope Baffle System

For the 1991 flight we installed a sunshade and a baffle system in the telescope. The sunshade shields both the instrument and the rocket ACS tracker from direct sunlight and the sunlit atmosphere. Without a sunshade, the tracker requires that the sun be 18° below the horizon viewed from an altitude of 300 km. This requires the solar zenith angle to be greater than 135° (45° below the horizon viewed from the earth's surface). With the sunshade and baffles installed, we can observe targets within 18° of the sun during daytime.

The sunshade is a 45 cm diameter cylinder cut by a plane which is tilted by 15° with respect to the telescope optic axis. The overall length of the sunshade is 1.9 m. During launch it is stowed along the outside of the telescope tube. After the rocket motor and instrument separate during flight, two motor driven screws extend the shade. They also retract it before reentry.

In flight, the instrument is oriented in roll so that the sunshade presents its longest side to the sun. A secondary knife edge baffle mounted on the sunshade insures that the sunshade edge, which is illuminated by direct sunlight, is shielded from the fields of view of the ACS tracker and the telescope for elongation angles of 18° or larger. Additional baffles placed inside the telescope and on the tracker shield their fields of view from the inside surface of the sunshade. These additional structures are required because parts of the inside of the sunshade can be illuminated by sunlight reflected from the earth during observations made when the ecliptic plane is not perpendicular to the horizon.

Observations

Rocket 27.110 on September 15, 1988

We observed Venus from rocket 27.110 launched at White Sands Missile Range, N.M. on September 15, 1988 at 10.0 Hrs UT approximately 24 days after its greatest Western elongation which occurred on August 22, 1988. Table II and Fig. 1 summarize the parameters for both the 1988 and 1991 observations.

The spectrograph entrance slit for the 1988 flight was 0.01 x 1.59 mm corresponding to an angular scale of 0.9 x 137 arc seconds. We chose the roll orientation of the rocket so that the long dimension of the slit was parallel to the Venus - Sun line. The IMSS acquired Venus at T+130 sec and stabilized its image on the entrance slit for a total of 380 sec. During that time we used the slit jaw TV camera and ground commands to scan the image of the planet across the entrance slit in discrete steps. We began by positioning the slit on the equator. After an initial 10 sec integration we stepped the image north until the slit was about 2 arc seconds below the south pole and then south until the slit was located at approximately +40° latitude stopping for a 10 sec measurement every 0.75 arc seconds of image motion. At T+480 sec, we returned to the equator for a final observation.

After the flight, we analyzed the TV camera images to determine the latitude of the slit on the planet for each observation. We determined that the uncertainty in slit position is 0.5 step = 0.38 arc seconds. This angular uncertainty corresponds to a 2.3° uncertainty in latitude for observations made at the equator, increasing to 9.5° at high latitude (80°).

The uncertainty in position is small compared with the spatial resolution of our observations. Based on laboratory measurements, the image of a 0.5 arc second diameter source has a full width half maximum of 1.5 arc seconds in the focal plane of the telescope. Flight IMSS error sensor signals indicate that the uncompensated jitter in the image was 1 arc second peak to peak. These two effects increase the projected slit width from 0.9 arc seconds to about 3 arc seconds, corresponding to a spatial resolution of 18.4° in latitude at the equator.

Rocket 36.078 on March 29,1991

We observed Venus from rocket 36.078 on March 29, 1991 at 2.5 Hrs UT, approximately 76 days before its greatest Eastern elongation which occurred on June 13, 1991. This observation was the first part of an experiment to measure the middle ultraviolet spectrum of Venus (190 - 230 nm) and Mercury (200 - 310 nm) with 0.15 nm resolution. We chose the launch time so that the zenith angle of Mercury was 88.5°. This placed Venus at a zenith angle of 70.4° and the sun at a zenith angle of 104°; thus for altitudes above 195 km, the rocket was in sunlight.

The spectrograph entrance slit for this flight was 0.025 x 1.59 mm corresponding to an angular scale of 2.2 x 137 arc seconds. A new rocket ACS and improvements to the IMSS significantly reduced the uncompensated image jitter observed in 1988 resulting in an effective angular resolution of 3.2 arc seconds. Again, we chose the roll orientation of the rocket so that the long dimension of the slit was parallel to the Venus - Sun line. The IMSS acquired Venus at approximately T+130 sec. A glitch in the rocket pointing required additional time for image stabilization. After approximately 10 sec, we positioned the entrance slit on the equator using ground commands where it remained for 50 sec.

At T+180 sec, the rocket ACS pointed the instrument toward Mercury. The IMSS briefly acquired Mercury, but before it could stabilize the image the ACS tracker lost contact with Mercury and was not able to reestablish it. No spectral data were acquired from Mercury. A post flight analysis suggests that the ACS star tracker was confused by debris which entered its field of view.

Reflectance Spectra

Method

The reflectance relates the observed radiance of a planetary atmosphere, I, to the incident solar irradiance, F, through the relation $I = R \cdot F/\pi$. Typical units for atmospheric radiance and solar irradiance are photons per area per steradian per second per wavelength interval, $I(photons/cm^2 \cdot str \cdot sec \cdot nm)$, and photons per area per second per wavelength interval, $F(photons/cm^2 \cdot sec \cdot nm)$, respectively. (A common practice is to include a factor of π in the definition solar irradiance and to write $F = \pi \cdot f$ and $R = I/f$).

Figure 2 shows examples of equatorial observations obtained during September 1988 (lower curve) and March 1991. For these plots, we binned the detector output by a running sum of five and resampled the result on 0.1 nm wavelength centers to produce spectra with 0.2 nm resolution. Derivation of the reflectance spectrum from these data requires knowledge of the instrument absolute radiometric calibration. If $D(\lambda)$ and $Cal(\lambda)$ are the detected count rate corrected for scattered light and background and the absolute calibration respectively, then

$$R = \frac{\pi \cdot D(\lambda) \cdot Cal(\lambda)}{F_E(\lambda)/r_V^2} \qquad (1)$$

where $F_E(\lambda)$ is the solar irradiance at 1 AU, and r_V is the heliocentric distance to Venus in AU. Examples of reflectance spectra calculated from our observations using Equation 1 and a solar spectrum obtained in 1985 by Van Hoosier *et al.* (1988) using the Solar Ultraviolet Spectral Irradiance Monitor (SUSIM) on board Spacelab 2 appear in Fig. 3 and Fig. 4. Figure 3 compares equatorial spectra from the two flights. Figure 4 compares the September 1988 equatorial spectrum shown in Fig. 3 with mid latitude (35°) and high latitude (55°) spectra taken on that same date.

Accuracy of the Derived Reflectance Spectra

The accuracy of the spectra shown in Fig. 3 and Fig. 4 is affected by uncertainty in the solar irradiance and errors in our observations and calibration. Van Hoosier *et al.* quote an uncertainty of 5% for their solar irradiance measurement made in 1985. Additional uncertainty on the order of 3% results from solar cycle variations (Lean 1989). In the following paragraphs we discuss the errors in our observations and calibration.

Since the CODACON detects the arrival of individual photons, we estimate the standard deviation of the measurement at each wavelength to be equal to the square root of the number of observed counts. Typical values of the random errors in reflectance which result from photon noise are shown in Fig. 4 for the 1988 observations and in Fig. 5 for the 1991 observations.

We also corrected the data for two potential systematic errors: detector dead time and spectrograph scattered light. In a pulse counting detector the true count rate is related to the observed count rate by the equation:

$$C_T = \frac{C_o}{1 - \tau \cdot C_o} \qquad (2)$$

where τ is the detector dead time. For the CODACON, (τ=3.5x10^{-6} sec) the dead time correction varies from 0.5% for the high latitude September 1988 observations to 8.2% for the March 1991 observations. We also subtracted a scattered light signal from the data. Both the solar irradiance and the reflectance of the atmosphere decrease toward shorter wavelengths. Below 192 nm the observed spectrum no longer decreases. We used this residual signal (See the dotted curves in Fig. 2) as the scattered light correction.

In order to determine $Cal(\lambda)$ in Equation 1, we must measure the absolute sensitivity of the spectrograph and the effective area (product of geometrical area and the square of its mirror reflectivity) of the telescope. For rocket 27.110, we used a deuterium lamp (Walker *et. al.* 1988) which was calibrated at the National Institute for Standards and Technology (NIST) as an irradiance standard for determining the absolute sensitivity of the spectrograph. We calculated the telescope effective area using telescope layout drawings, laboratory measurements, and reflectivities provided by the mirror coating vendor. For rocket 36.078 we used a deuterium lamp combined with a scattering screen coated with Eastman White Reflectance Standard (Grum and Wightman 1977) as radiance standard. This allowed us to directly measure $Cal(\lambda)$ for the assembled telescope-spectrograph. We found that using the lamp and screen as a radiance standard resulted in a calibration which is more certain than one obtained using only the lamp as an irradiance standard. Table III summarizes the accuracy of the determination of $Cal(\lambda)$ for the two flights. The magnitudes of our calibration error estimates are shown above the two reflectance curves in Fig. 3. They are composed of a wavelength independent component (e.g. telescope area and measured distances) and a wavelength dependent component (e.g. atmospheric absorption and lamp intensity). These two components are statistically independent and combine in quadrature to produce the total uncertainty. The wavelength dependent error estimates are identical for both calibrations and result largely from our imprecise knowledge of atmospheric absorption. The wavelength independent errors are the dominant components for wavelengths greater than 200 nm. They

cause the absolute values of the derived reflectances to be uncertain by 16% and 9% for the 1988 and 1991 observations respectively.

Combining the uncertainties in solar irradiance and our calibration produces a formal estimate of the uncertainty in the absolute value of the reflectance for wavelengths greater than 200 nm equal to 17% and 11% for the two flights.

Discussion

Figure 5 compares the reflectance spectrum from the 1991 flight with an SO_2 absorption spectrum calculated using cross sections from Freeman *et. al.* (1984) and a column density of 5×10^{16} cm^{-2}. There is an obvious line by line correspondence between the two spectra, confirming the identification of SO_2 as a primary absorber over the entire wavelength range. Except for a missing band at 205 nm, the shapes and positions of individual bands match in detail for wavelengths less than 210 nm. Above 210 nm the strengths of the bands suggest an increasing equivalent absorbing column of SO_2. These stronger bands indicate that a simple model in which SO_2 is uniformly mixed with a featureless wavelength dependent absorber (e.g. CO_2) does not fit the observations. This conclusion is also supported by the results presented in Fig. 4 which show that the spectrum flattens and the SO_2 bands weaken at high latitudes (at greater incidence and emission angles).

In addition to the discrepancy in band strengths, the Venusian spectrum also contains a number of additional features above 210 nm. We have used synthetic spectra to investigate the possibility that some of these features are artifacts which result from using separate instruments to observe Venus and the sun. Our results are summarized in Fig. 6. The lower curve is a hypothetical reflectance spectrum generated from a laboratory SO_2 absorption spectrum with a wavelength dependent column density multiplied by a continuum curve. The middle curve in Fig. 6 shows the reconstruction of the hypothetical reflectance spectrum from a synthetic planetary spectrum. We generated the planetary spectrum in two steps. First we multiplied the lower curve in Fig. 6 by the SUSIM solar spectrum. Next, we multiplied that result by our instrument calibration curve and the integration time from the 1991 flight, adding photon noise with a random number generator. The result was a SUSIM generated planetary spectrum which simulates the 1991 observations shown in Fig. 2. We then used Equation 1

with the SUSIM solar spectrum in the denominator to produce the middle curve. Since we used the SUSIM spectrum in the synthesis and reconstruction, the derived reflectance spectrum is independent of instrument calibration and the differences in the two lower curves arise from random errors caused by photon noise. The upper curve in Fig. 6 was also derived from our SUSIM generated planetary using equation 1 except, in the denominator we used a solar spectrum obtained from the Solar-Stellar Irradiance Comparison Experiment (SOLSTICE, Rottman *et. al.* 1993) aboard the Upper Atmospheric Research Satellite. Differences in the middle and upper curves result entirely from differences in the SUSIM and SOLSTICE spectra. Below 210 nm the solar spectrum is relatively featureless and small differences in SUSIM and SOLSTICE spectra do not significantly alter the reconstructed reflectance spectrum. On the other hand, above 210 nm small differences in SUSIM and SOLSTICE produce artifacts which are comparable in size to some of the additional features seen in Fig. 5.

Photochemical models predict a number of carbon and sulfur compounds are formed above the clouds from reactions of CO_2 and H_2SO_4 (Krasnopol'sky and Parshev, 1983). Na *et. al.* (1990) have demonstrated that SO is present above the cloud tops by showing that atmospheric models including both SO and SO_2 fit their IUE spectra more closely than models which contain only SO_2. In a following paper Na *et. al.* (1994) use the observations reported here to refine their determination of SO and to derive the spatial distribution of SO_2 above the cloud tops in 1988. In principle, absorption spectroscopy can be used to infer the altitude distribution of additional trace species; however, the measurements are complicated by the ubiquitous presence of SO and SO_2. Our simulation shows that accurate identification and measurement of additional species require observations in which both the planetary radiance and the solar irradiance are measured during a single observing sequence with the same instrument.

Conclusions

Rocket observations of the near ultraviolet spectrum of Venus show that SO_2 is the primary spectral absorber in the wavelength range 190 - 230 nm. In a following paper Na *et. al.* (1994) show that SO features are also present in these data. Accurate identification of additional species in this

wavelength range will be most accurately accomplished using an instrument which can view both the planetary radiance and the solar irradiance.

The current rocket observations are more useful than IUE data for constraining the distribution of SO and SO_2 above the clouds on Venus. Na *et al.* (1990) estimate that a typical pointing uncertainty of 3 arc seconds for an IUE observation results in a factor of 2 error in the derived SO_2 abundance. Absolute pointing errors for the rocket are less than 0.4 arc seconds. Also, the higher signal to noise ratio of the rocket observations permits a more accurate determination of SO abundance than is possible with IUE (Na *et. al.* 1994).

Future rocket experiments have three additional advantages over those which can be performed using earth orbiting instruments. First, the rocket instrument can be modified to obtain both a planetary radiance spectrum and a solar irradiance spectrum during a single flight. Second, spatially resolved spectra obtained during 1988 indicate that the range of altitudes probed by 190 - 230 nm spectra is very sensitive to incidence and emission angle. IUE and the Hubble Space Telescope (HST) observations are restricted to phase angles within a narrow range centered on 90° (when solar elongation angles are $\geq$ 45°). On the other hand, the rocket instrument can observe Venus whenever the solar elongation angle is $\geq$ 18° providing a phase angle coverage of 25° - 155°. Finally, satellite observations are restricted to two short periods of time near greatest Eastern and Western elongation every 19 months while the rocket instrument can observe Venus over 70% of its orbit. Therefore, the rocket instrument is much more useful than IUE or HST for observing transient atmospheric events.

Acknowledgment

This research was supported the National Aeronautics and Space Administration under research grant NSG 5103.

References

Barker, E. S. 1989. Detection of SO_2 in the UV spectrum of Venus. *Geophys. Res. Lett.* **6,** 117-120.

Bottema, M. and R. A. Woodruff 1979. Third order aberrations in Cassegrain-type telescopes and coma correction in servo-stabilized images. *Appl. Optics* **10,** 300-303.

Conway, R. R., R. P. McCoy, C. A. Barth, and A. L. Lane 1979. IUE detection of SO_2 in the atmosphere of Venus. *Geophys. Res. Lett.* **6,** 629-631.

Freeman D. E., K. Yoshino, J. R. Esmond, and W. H. Parkinson 1984. High resolution absorption cross section measurements of SO_2 at 213° K in the wavelength region 172-240 nm. *Planet. Space Sci.* **32,** 1125-1134.

Grum, F. and T. E. Wightman 1977. Absolute reflectance of Eastman White Reflectance Standard. *Appl. Optics* **11,** 2775-2776.

Krasnopol'sky, V. A. and V. A. Parshev 1983. Photochemistry of the Venus atmosphere, in *Venus*, edited by D. M. Hunten *et. al.*, p. 431. University of Arizona Press, Tucson.

Lean, J. 1989. Contribution of ultraviolet irradiance variations to changes in the Sun's total irradiance. *Science* **244,** 197-200.

McClintock, W. E., C. A. Barth, R. E. Steele, G. M. Lawrence, and J. G. Timothy 1982. Rocket-borne instrument with a high-resolution microchannel plate detector for planetary UV spectroscopy. *Appl. Optics,* **21,** 3071-3079.

Na, C. Y., L. W. Esposito, and T. E. Skinner 1990. International Ultraviolet Explorer Observation of Venus SO_2 and SO. *J. Geophys. Res.* **95 ,** 7485-7491.

Na, C. Y., L. W. Esposito, W. E. McClintock, and C. A. Barth 1994. Sulfur dioxide in the atmosphere of Venus II. Modeling Results. *Icarus*, this issue.

Rottman G. J., T. N. Woods, and T. P. Sparn 1993. Solar-Stellar Irradiance Comparison Experiment I 1. Instrument Design and Operation. *J. Geophys. Res.* **98,** 10667-10677.

Stewart, A. I. F., D. E. Anderson, L. W. Esposito, and C. A. Barth 1979. Ultraviolet spectroscopy of Venus: Initial results from the Pioneer Venus Orbiter. *Science* **203,** 777-778.

Van Hoosier, M. E., J. F. Bartoe, G. E. Brueckner, D. K. Prinz 1988. Absolute solar irradiance 120 nm- 400 nm. *Astrophys. Lett.* **27,** 163-168.

Walker, J. H., R. D. Saunders, J. K. Jackson, and D. A. McSparron 1988. The NBS scale of spectral irradiance, *J. Res. Natl. Bur. Stand.* **93(12),** 7-20.

Zasova, L. V., V. I. Moroz, L. W. Esposito, and C. Y. Na 1993. SO2 in the middle atmosphere of Venus: IR measurements from Venera-15 and Comparison to UV data. *Icarus* **105,** 92-109.

Table I

Instrument Summary

Parameter		Value
Telescope	Tilted Aplanat	
	Focal Length	240 cm
	Aperture	39 cm
	Spatial Resolution	1 arc sec FWHM
	Focal Plane Scale	11.5 μm/arc sec
Spectrograph	Ebert-Fastie	
	Focal Length	25 cm
	Grating	2400 g/mm
	Coverage	38.5 nm
	Spectral Resolution	0.2 nm
Detector	CODACON microchannel plate	
	Anode	Coded Array
	Number of Channels	1024
	Channel Spacing	0.025 mm

Table II
Observation Summary

	27.110	36.078
Date	September15, 1988	March 29,1991
Solar Elongation	44.3° West	34.6° East
Phase Angle	76.5°	51.6°
Illumination	62%	82%
Angular Diameter	18.8"	13.3"
Spatial Resolution (angular)	3"	3.2"
Spatial Resolution (latitude)	±9.2° at Equator ±22° at 68° South	±14° at Equator

Table III
Calibration Error Estimates

Rocket 27.110

Wavelength (nm)	190	195	200	210	220	230
Standard Lamp	11.2%	9.1%	9.1%	7.1%	7.1%	7.1%
Atmospheric Absorption	10.6%	5.3%	1.8%	1.4%	1.0%	0.7%
Instrument Parameters	14.0%	14.0%	14.0%	14.0%	14.0%	14.0%
Total R. M. S. Error	21%	18%	17%	16%	16%	16%

Rocket 36.078

Wavelength (nm)	190	195	200	210	220	230
Standard Lamp and Screen	11.9%	9.8%	9.7%	7.8%	7.8%	7.7%
Atmospheric Absorption	10.6%	5.3%	1.8%	1.4%	1.0%	0.7%
Instrument Parameters	3.4%	3.4%	3.4%	3.4%	3.4%	3.4%
Total R. M. S. Error	16%	12%	10%	9%	9%	8%

FIGURE CAPTIONS

Figure 1. Local horizon views of Venus as seen from White Sands Missile Range, NM. on the two observation dates. The entrance slit of the spectrograph, which was aligned with the Venus-sun line, is shown against the planet's disk. During the September 15, 1988 observations, we scanned the image of the planet north and south across the slit using ground commands. During the March 29, 1991 observation the slit was held fixed on the equator. The equivalent projected slit width for both observations was about 3" resulting in a latitude resolution at the planet's equator of 18.4° and 28° respectively.

Figure 2. Examples of the equatorial observations obtained in September 1988 (lower curve) and March 1991 (upper curve). The ordinate is detector counts per 0.2 nm. Dotted curves mark the levels of a scattered light signal which were subtracted from each observation.

Figure 3. Reflectance spectra derived from the two observations shown in Figure 2. Error bars above the plots represent the uncertainty in the instrument calibration. Combining the uncertainties in solar irradiance and instrument calibration produces formal estimates for the absolute value of these two spectra which is only slightly larger than the uncertainties due to the calibration alone.

Figure 4. Comparison of equatorial, mid latitude, and high latitude reflectance spectra derived from the 1988 flight. The equatorial and mid latitude curves have been displaced upward by 0.2 and 0.1 for clarity. Error bars show typical values of the random errors in reflectance which result from photon noise.

Figure 5. Comparison of the reflectance spectrum obtained on March 1991 with an SO_2 absorption spectrum calculated using a laboratory cross section and a column density of 5×10^{16} cm^{-2}. The error bars represent typical values of the random errors in reflectance which result from photon noise.

Figure 6. Synthetic spectra illustrating that spurious spectral features can arise in reflectance spectra when separate instruments are used to observe the planetary radiance and the solar irradiance. The lower curve is a hypothetical reflectance spectrum of a planetary atmosphere containing SO_2. The middle curve is the reflectance spectrum derived from a simulated measurement of this hypothetical spectrum using the same instrument to observe the planet and the sun. The upper curve was

derived from a simulation in which different instruments were used to observe the planet and the sun. Differences in the upper two curves result entirely from differences in the solar spectrum measured by the two instruments.

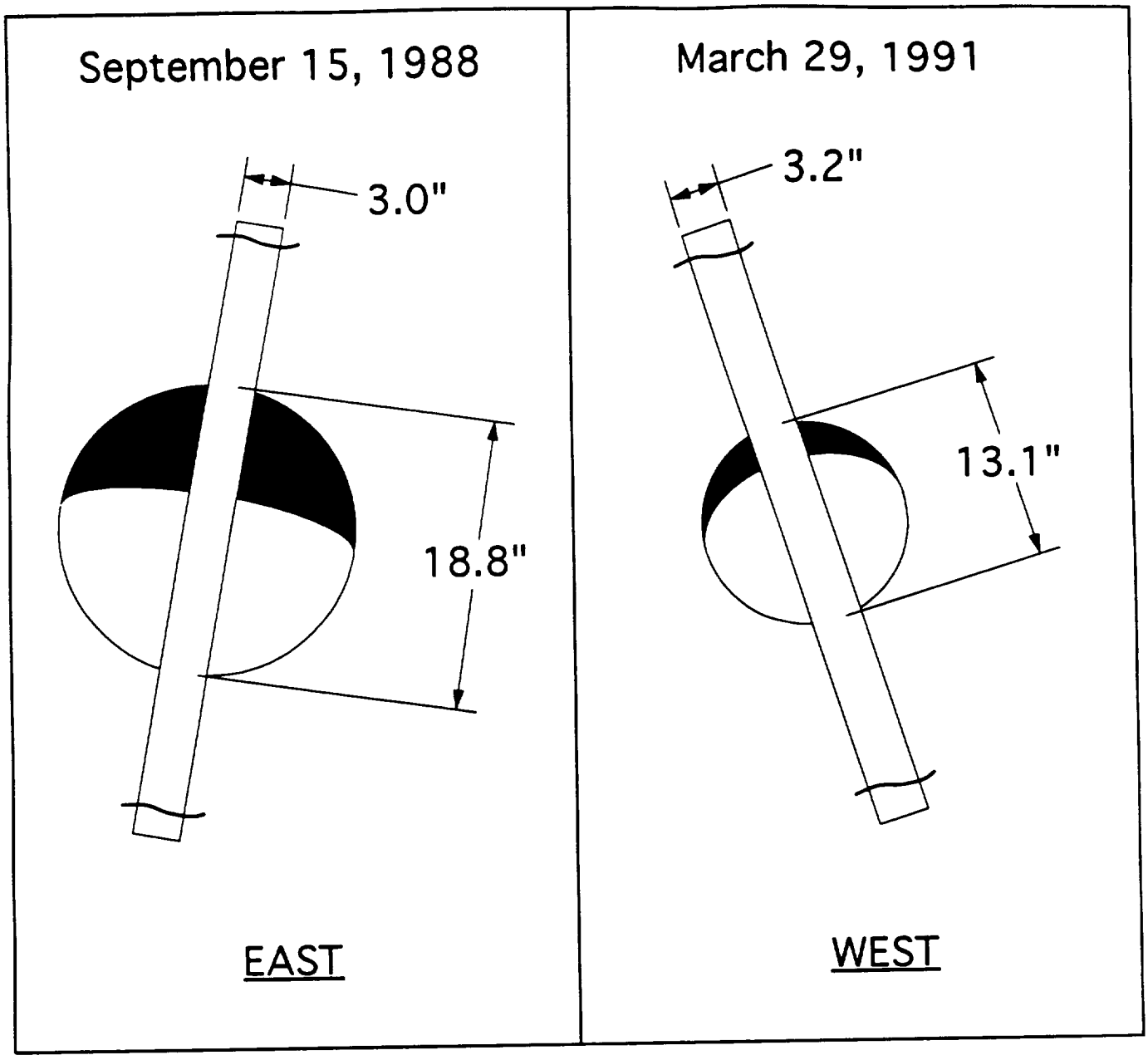

FIG 1

McC[illegible] et al

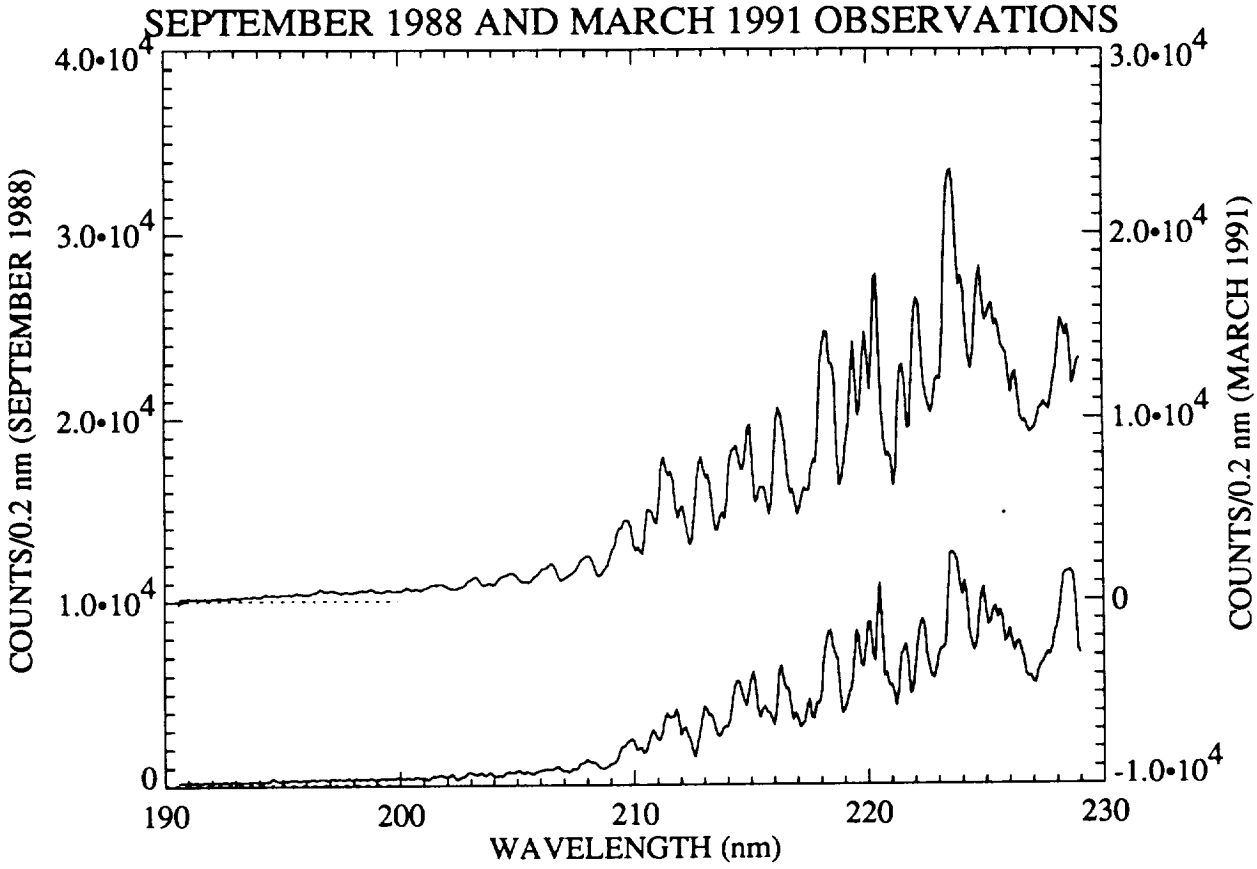

FIG 2
McClintock et-al.

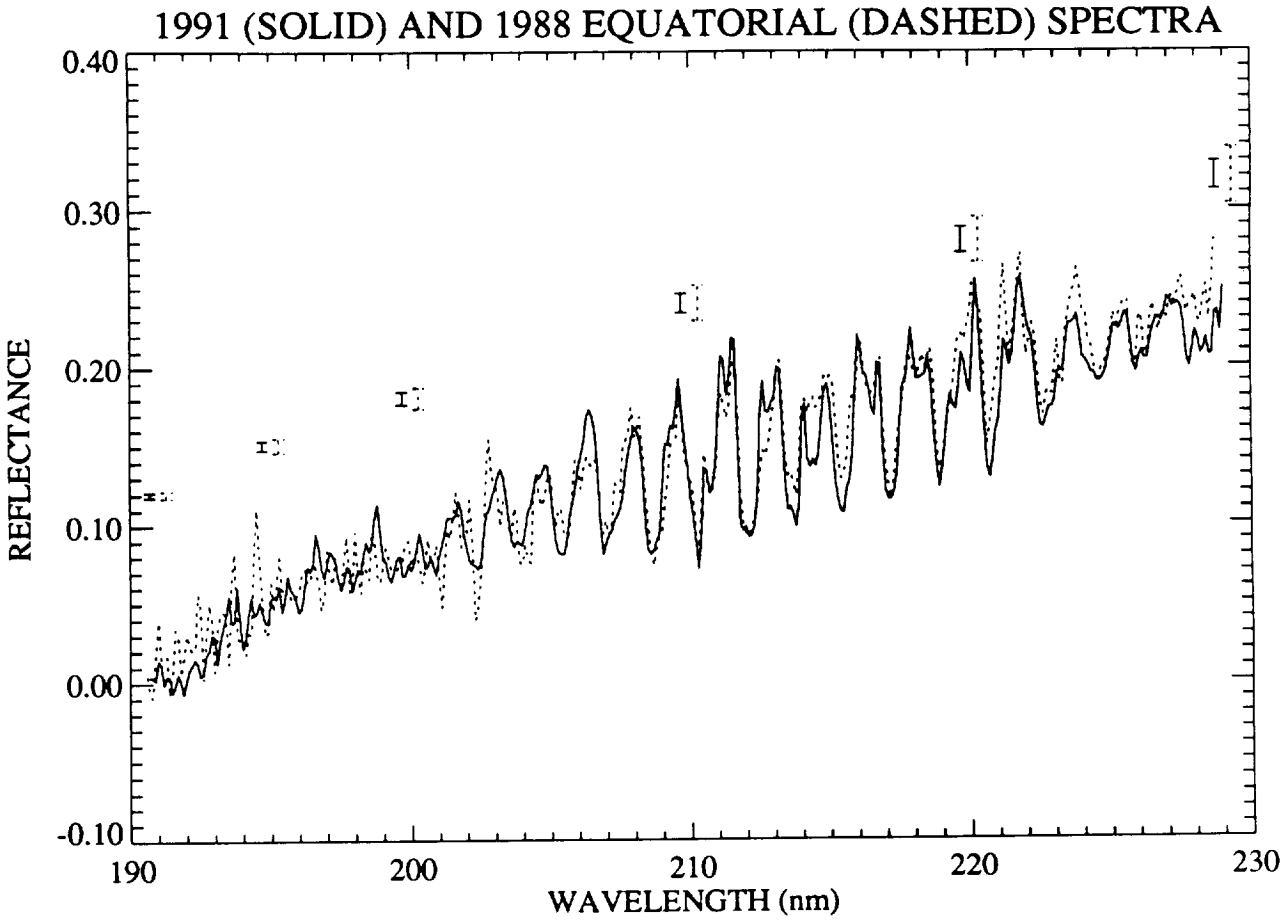

FIG 3

McCLINTOCK et. al.

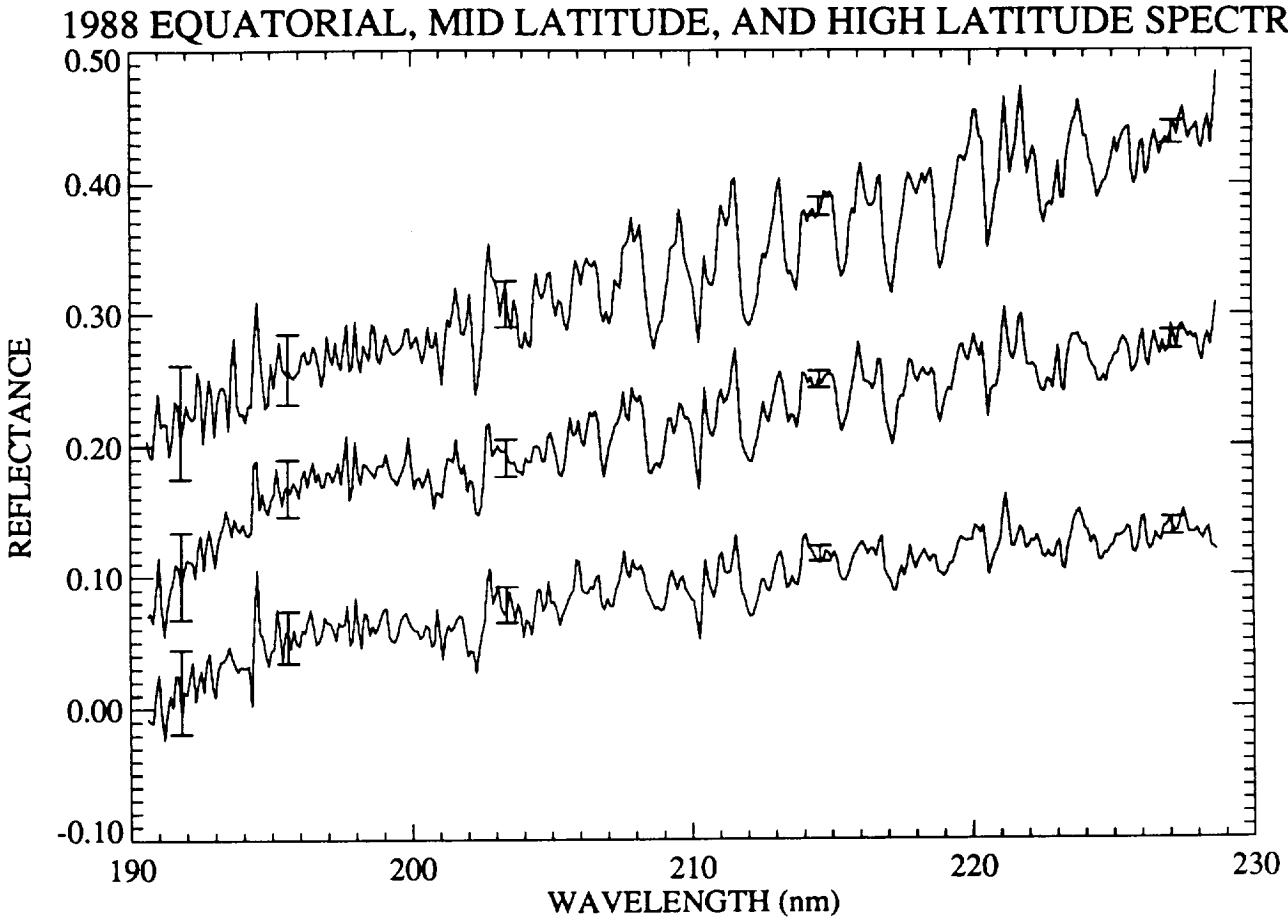

FIG 4

McCLINTOCK et. al

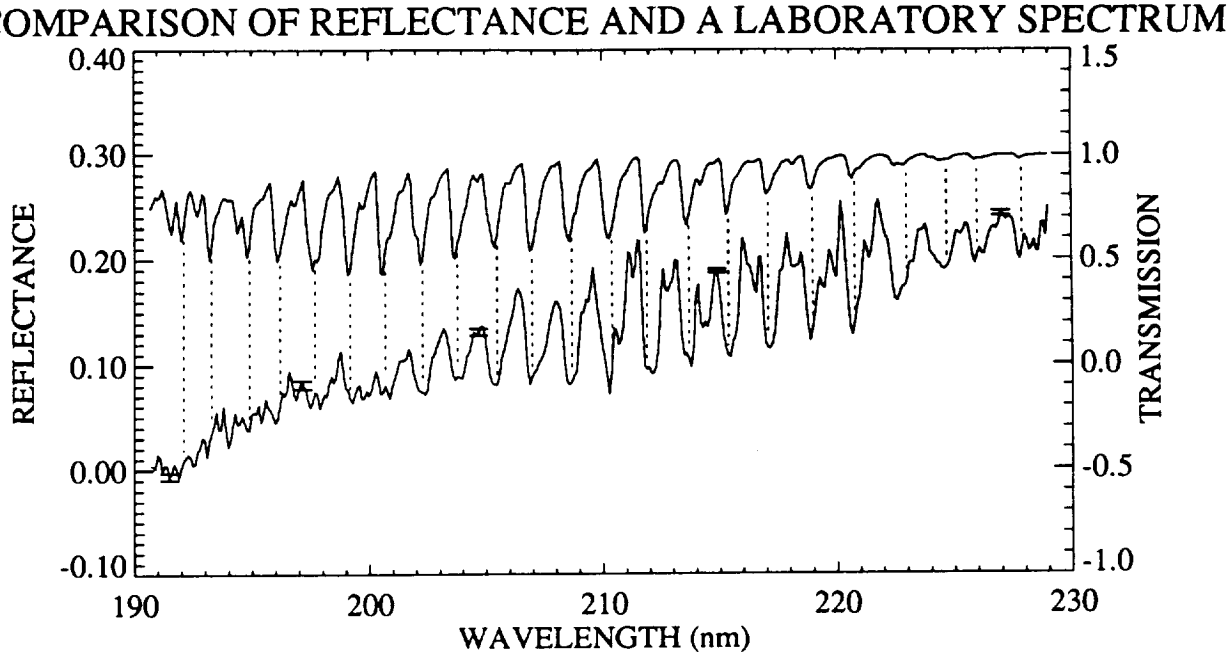

Fig 5

McClintock et.al.

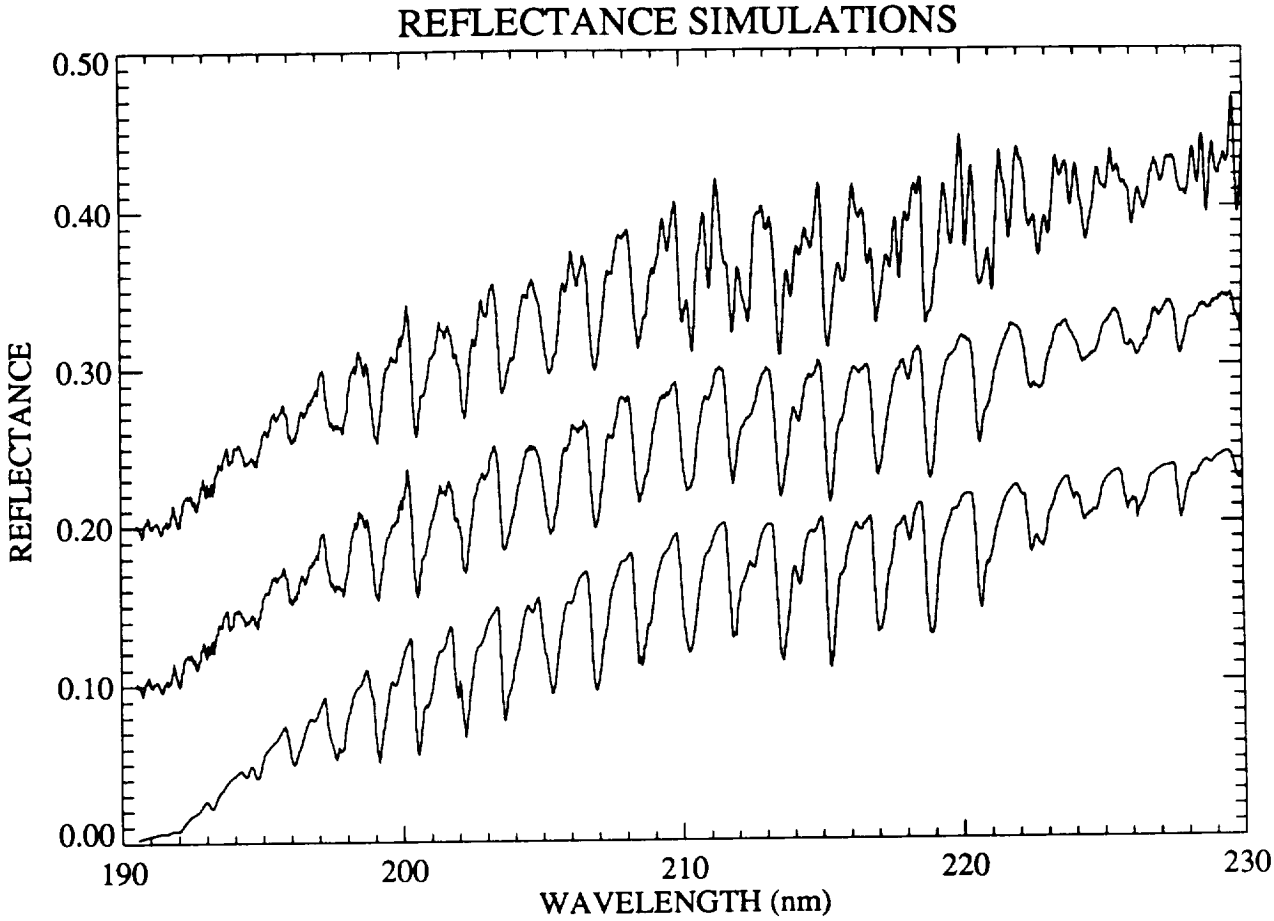

FIG 6

McCLINTOCK et.al.

March 11, 1994

Sulfur Dioxide in the Atmosphere of Venus:

II. Modelling Results

C. Y. Na[1], L. W. Esposito, W. E. McClintock, C. A. Barth

Laboratory for Atmospheric and Space Physics

Campus Box 392

Boulder, Colorado 80309

[1]Southwest Research Institute

P. O. Drawer 28510

San Antonio, TX 78228

(210) 522-2848

chan@termite.space.swri.edu, SWRI::NA

12 pages

7 figures

2 tables

Keywords: Sulfur Dioxide, Venus, Atmosphere

Running Head: **VENUS SO_2 AND SO**

Chan Y. Na

[1]Southwest Research Institute

P. O. Drawer 28510

San Antonio, TX 78228

(210) 522-2848

chan@termite.space.swri.edu, SWRI::NA

Abstract

We report the results from UV sounding rocket observations of Venus made on 15 September 1988 and 29 March 1991 which obtained high resolution spectra of Venus clouds from 190 to 230 nm. The albedo of Venus in this wavelength range is dominated by absorption features of sulfur dioxide and sulfur monoxide. We estimate the mixing ratio of SO_2 above the clouds of Venus is 80±40 ppb for 1988 and 120±60 ppb for 1991. The scale height of SO_2 at the same altitude region is 3±1 km for both 1988 and 1991. These numbers are in good agreement with both Pioneer Venus and IUE observations made around the same time period, and indicate that no large change in SO_2 above the clouds occurred from 1982 to 1991.

In addition, the SO mixing ratio above the clouds derived from the 1991 observations is 10±5 ppb, and the scale height of SO above the clouds is close to that of the bulk atmosphere. Our analyses indicate that the mixing ratio of SO decreases sharply below the 64 km level. This vertical profile of SO derived from the rocket observation in 1991 is in good agreement with the photochemical models.

The mixing ratio of SO_2 at the cloud top level derived from the 1988 observation ranges from 60±30 ppb at the equator to 300±150 ppb near 50°S. The scale height of SO_2 at the cloud top region ranges from about 3-4 km at the equator to 1.5 km near 50°S. Venera 15 observations show similar latitudinal variation of SO_2.

Introduction

SO_2 was first detected in the atmosphere of Venus by Barker [1979] with ground-based observations, and it was subsequently confirmed by Stewart et al. [1979] and Conway et al. [1979]. These observations indicated that the abundances of SO_2 in 1978-1979 period were larger than the previously established upper limits [Owen and Sagan, 1972] by an order of magnitude. Continuous observations by Pioneer Venus from 1978 to 1986 showed a steady decline in the cloud top SO_2 abundance toward values consistent with previous upper limits [Esposito et al. 1988]. This decline has been confirmed by IUE observations [Na et al. 1990]. Explanations that have been advanced for the observed decline of SO_2 include active volcanism and changes in atmospheric dynamics.

The episodic nature of the change in SO_2 abundance led Esposito [1984] to conclude there was a significant injection of SO_2 into the Venus middle atmosphere prior to Pioneer Venus arrival at Venus. Esposito suggested the bouyant thermal flux from an immense volcanic eruption as a natural physical mechanism for the injection. The case for active volcanism in Venus' geologic past is supported by a number of arguments, including i) the Magellan orbiter observations of numerous volcanic features such as domes and lava flows [e.g., Head 1990, 1991]; ii) detections by both Pioneer Venus and Galileo of strong radio signals suggesting widespread and recurring lightning at Venus, particularly lightning associated with the mountainous regions [Ksanfomaliti, 1980; Scarf et al. 1980, Gurnett et al. 1991]; and iii) decline of SO_2 at the cloud top region of Venus observed by Pioneer Venus and IUE [Esposito et al. 1988, Na et al. 1990].

However, the evidence of lightning associated with mountainous regions on the planet's surface has been challenged by Taylor and Cloutier [1986], who suggested SO_2

variation could be explained in terms of changes in atmospheric circulation. This explanation for the decline in SO_2 abundance had been considered by Esposito [1984] but rejected on the grounds that the time scale for atmospheric phenomena at the cloud tops is on the order of months, while the inferred injection event had a time scale of decades.

Based on the analysis of Pioneer Venus Cloud Photo-Polarimeter (OCPP) data, Del Genio and Rossow [1989] suggested that the cloud level dynamics may be cyclic with a time scale of 5-10 years. In addition, Clancy and Muhleman [1991] showed a similar time scale for the change in CO mixing profiles in the mesosphere of Venus. They suggested that the variation of CO and the decline of SO_2 are related phenomena, and that the decline of SO_2 could be explained without invoking active volcanism.

Furthermore, the changes in SO_2 above and within the clouds of Venus may have a significant effect on the photochemistry of the clouds of Venus. Pioneer Venus observations have shown that the clouds of Venus are created by the photochemical processes that oxidize upwelling SO_2 [Winick and Stewart 1980, Yung and DeMore 1982]. Thus, any significant changes in SO_2 may have sn effect on the chemistry and dynamics of the clouds. In this paper, we present the results from two sounding rocket observations of Venus made in the wavelength range 190-230nm [McClintock et al. 1994]. Our objectives are 1) to extend the timebase of observations to look for changes in SO_2 abundance in the Venus atmosphere, 2) to observe Venus with a high spatial resolution to study the horizontal variations of SO_2 above the clouds, 3) to provide a check on the results of Pioneer Venus and IUE by making independent measurements of SO_2 abundance, and 4) to search other UV absorbers such as SO, OCS and CS_2 which are important in constraining the photochemical studies of Venus atmosphere.

Observations

Rocket observations of Venus were made on 15 September 1988 and 29 March 1991. The first observation was made 24 days after greatest Western elongation of Venus, and the phase angle of of Venus was 76.5°. The disk of Venus at the time subtended an angular diameter of 18.8″, and the defect of illumination was 38% (Fig. 1). The second observation was made on 29 March 1991 when the phase angle of Venus was 51.6°. The disk of Venus at the time of observations was 13.1 arc seconds wide and the defect of illumination was about 18% (see Table 1).

The CU/LASP planetary rocket payload consists of a Cassegrain type telescope and an Ebert-Fastie spectrograph equipped with a CODACON microchannel plate detector. The detector has 1024 elements, and provides a spectral coverage of approximately 375 Å with a spectral resolution of 2 Å. A detailed description of the spectrograph performance can be found in McClintock et al. [1982, 1994].

Pointing of the rocket telescope is accomplished by a star tracker located in front of the secondary mirror of the telescope. The star tracker points the telescope to within 1 to 2 arc minutes of the target, and more precise pointing (1-2″) is achieved by an Internal Motion Compensation System. The 1988 observations included a succession of spatially resolved spectra of Venus. In 1991, data were taken from a single pointing centered on the equator of Venus [see Paper I].

Analysis

Model Procedure

The model atmosphere of Venus, which is based on the ground-based and Pioneer Venus observations, is composed of CO_2 gas and sulfuric acid aerosols which are mixed uniformly with the gas from about the 50 km to the 80 km level. The aerosols have a radius of about 1 μm and are assumed to have a single scattering albedo of 0.98 [Kawabata and Hansen, 1975]. In addition, a pure absorbing layer with an optical depth of 0.2 is added at an altitude of 75 mbar [Esposito 1979]. Then, absorbers such as SO_2 and SO are added to the clear atmosphere with distributions given by two parameters, the mixing ratio and scale height at the cloud top (40 mbar). Table 2 lists the range of values for the parameters used in the present analysis.

After the absorbers are added to the model atmosphere, the optical depth, single scattering albedo, and Rayleigh scattering fraction are calculated at each wavelength. These values are then used by a multiple scattering radiative transfer code based on the Markov chain method [Esposito and House 1978, Esposito 1979] to calculate the model brightness. The model spectra are calculated at 2 Å intervals which is the effective wavelength resolution of the rocket spectrograph. We derived the mixing ratio and the scale height of SO_2 by choosing the models that minimize the root mean square (RMS) differences between model spectra and the rocket data.

Observing geometry

As shown in Fig. 1, the entrance slit covers the entire length of disk of Venus in one dimension, therefore the flux reaching the detector is from an entire latitudinal zone of Venus. Within that latitudinal zone, the solar zenith angles and the observation angles

vary greatly. Thus, modelling of this flux through the slit involves dividing the latitudinal zone of Venus into small areas where the observing geometry is assumed constant. At the center of each area, the local solar zenith angle and the observation angle are calculated, and are used in the model calculation. The intensity for the entire latitudinal zone is the average of the intensities calculated at the center of the small areas.

Rapidly varying geometry near the limb introduces uncertainty, and it can be reduced by making each area small enough. To determine the optimum number of areas, we track the difference in brightness caused by each finer subdivision:

$$I_N - I_{N-1} < \epsilon \ \ where \ \ I_N = \frac{\sum_{i=1}^{N} I_i}{N}$$

I_N is the intensity for the entire laititudinal zone calculated with N number of areas. The calculation is repeated until the difference (ϵ) between I_N and I_{N-1} becomes less than 10^{-5}.

The entrance slit used for the 1991 observation was wider than the slit used for the 1988 observation. Combined with the smaller angular diameter (13″) of the disk of Venus at the time of observation, the entrance slit projected a much larger area on the disk of Venus. Since the slit covered more than 20 degrees in latitude of Venus, we divided the equatorial area of Venus projected by the slit into three strips, and on each of these three strips we repeated the analysis as described above. The model intensity for the observation is obtained by averaging the intensities from all three strips.

Results

Cloud top abundance of SO_2

The derived mixing ratio of SO_2 at the cloud tops was 80±40 ppb for September 1988, and 120±60 ppb for March 1991 observations. The scale height of SO_2 at the same altitude was 3±1 km for both 1988 and 1991 observations. The mixing ratio and scale height of SO_2 in 1988 represents the average value from all latitudes. The SO_2 abundance derived from two separate rocket experiments agrees well with the results from Pioneer Venus [Esposito et al. 1988] and IUE observations [Na et al. 1990] made around the same time period. As shown in Fig. 2, the SO_2 mixing ratios derived from four different instruments show remarkably good agreement: they all overlap within their respective error bars. It is clear from the Fig. 2 that the SO_2 abundance above the clouds has not experienced any large change from 1982 to 1991, and the mean abundance of SO_2 above the clouds is around 100 ppb.

Vertical profile of SO

Figure 3 shows the 1991 rocket spectrum and the model spectra, and it is clear the model that includes SO is much better fit than the model containing just SO_2. Since SO absorption features are embedded within the prominent SO_2 absorption features, a detailed modeling of SO requires data to have a high spectral resolution and a high signal to noise ratio (SNR). The SNR of the rocket data is much higher than the data from either Pioneer Venus and IUE due to higher sensitivity and greater dynamic range of the rocket instrument. This high SNR of the rocket data together with a high spectral resolution allowed a much more detailed analysis of SO in the Venus atmosphere.

In the analysis of IUE data [Na et al. 1990], SO was limited to the top 10 layers in

the model atmosphere, and was assumed well mixed with the atmosphere. In the present analysis, the number of layers that contain SO was varied as well as its mixing ratio and scale height at 40 mbar. First, we put SO in the top 10 layers in the amount determined by the mixing ratio and the scale height at 40 mbar level. Next, we increased the number of layers containing SO, and at each increment, we varied the mixing ratio and the scale height of SO. The best fit to the data was obtained when the model atmosphere had 12.5 ppb of SO with its scale height close to that of the bulk atmosphere down to about 64 km in altitude. Thus, we conclude that SO is well mixed with the atmosphere above ~ 64 km, and below 64 km, the mixing ratio of SO is greatly diminished. Figure 4 shows the derived vertical profile of SO from the 1991 observations along with the vertical profiles of SO from photochemical models by Winick and Stewart [1980] and by Yung and DeMore [1982]. It shows that the derived SO profile is in good agreement with the models. The SO mixing ratio of 15 ± 5 ppb above 64 km level is in good agreement with the value derived from the IUE observation [Na et al. 1990], and it is also consistent with the upper limits established from ground based observations by Wilson et al. [1981].

Latitudinal variation of SO_2

The observation carried out in September of 1988 made a vertical scan of the disk of Venus in sub-arcsecond steps. The derivation of SO_2 abundance was carried out for each of the steps by direct comparison with the model spectra. As shown in Fig. 5, there is a sizable variation in the abundance and scale height of SO_2 with latitude. The SO_2 mixing ratio is at a minimum near the equator (60 ± 30 ppb) and increases with latitude in both directions (300 ± 150 ppm at 50°S). The scale height of SO_2, on the other hand, decreases with latitude from about 4 km near the equator to ~ 2.5 km near 50°S.

We note that the derived value of the SO_2 mixing ratio at high latitudes could be influenced by uncertainty in the pointing of the telescope. However, it is estimated that the pointing was accurate to $\sim 0.4''$ during the flight. This small pointing error has negligible effect on the derived amount of SO_2 at low latitudes (<40°). Even at high latitudes, the pointing error much larger than $0.4''$ is required to have any significant effect on the derivation of the SO_2 abundance. In Fig. 6, the brightness of Venus at 2100 Å is plotted against latitude along with five models. The models have different SO_2 mixing ratios, but the scale height was fixed at 3 km. As seen in the figure, the data within 40° latitude are well matched by the models that have 50 and 100 ppb of SO_2, whereas the data between 40° to 60° lie between models that have 250 and 500 ppb of SO_2. It is clear from the figure that the latitudinal variation of SO_2 cannot be explained by errors in pointing alone.

As was seen in Fig. 5, the latitudinal variation of the mixing ratio of SO_2 and its scale height seems to be anti-correlated. At low latitudes, the scale height of SO_2 is at maximum while the mixing ratio is at a minimum. The variation of SO_2 above the clouds may be due to differences in atmospheric mixing above the clouds. The larger scale height of SO_2 around the equatorial region indicates that atmospheric mixing is more vigorous there than at the mid latitude region. This suggests that there is a hadley cell circulation right at the cloud tops. Comparison with Venera-15 observations described below support this idea.

Comparison with Venera-15 observations

The Fourier spectrometer on board Venera-15 made the first detection of SO_2 in the infrared spectral region from the spacecraft [Zasova et al. 1993]. The Venera-15 spacecraft arrived at Venus in September 1983; the standard observing session lasted from October

12, 1983 to December 14, 1983. The infrared measurements were made along the viewing tracks which started at low latitudes, went through the north pole, and finished at low latitudes again. More than 1500 spectra were obtained for latitudes from 65°S to 87°N. There was one session with a special (non-nominal) spacecraft orientation, when the nadir observations of the equator were conducted [Zasova et al. 1993].

The IR observations by Venera-15 probe the altitude region from 58 km to 72 km depending on cloud scale height and SO_2 scale height. Thus the results from infrared experiment can be compared to the UV rocket observations which is sensitive above the clouds. Figure 7 shows the mixing ratio and scale height of SO_2 derived from the Venera-15 observation along with the results from our rocket observations. The results from both UV and IR observations were binned into latitudinal bins that are 15°wide to reduce the scatter in the data. As seen in the figure, both the IR and UV data show a large variation of SO_2 abundance with latitude. The variation of SO_2 seen in the IR data is even higher than seen by UV observations. The mixing ratio of SO_2 derived from the IR observations increases from about 20 ± 10 ppb in the equatorial region to about 400 ± 100 ppb at high latitudes.

The difference in mixing ratio of SO_2 between UV and IR observations may result from uncertainty in the absolute flux calibration for both experiments, and the fact that the observations are separated by about 6 years in time. However, the general dependence of SO_2 mixing ratio with latitude is similar for both UV and IR observations. On the other hand, the scale height of SO_2 derived from the UV and the IR observations show opposite behavior. The differences in scale height of SO_2 between the two experiments may be due to the different vertical profile of the cloud aerosol used in the model calculations. For UV

model calculations, the aerosol is assumed mixed uniformly with the bulk atmopshere at all latitudes. For the IR observations, the scale height of cloud aerosols was measured by Venera-15, and it was used in deriving SO_2 mixing ratio and scale height. Venera 15 saw a significant variation in cloud aerosol scale height at high latitudes [Zasova et al. 1993]. Thus, the differences in SO_2 abundance from UV and IR observations may be an indication that the Venus atmosphere is considerably more complex than the two parameter model atmospheres used in the present analyses.

Now that the Pioneer Venus is no longer operational and IUE and HST are limited to observing Venus only at its greatest elongations, the only instrument capable of regularly monitoring the UV absorbers in the Venus atmosphere is sounding rocket. SO_2 and SO are important indicators of cloud top dynamics, chemistry and possibly surface geological activity on Venus as well. Regular observations are vital in documenting any long term changes in SO_2 and SO above the clouds of Venus and in understanding the physical mechanism responsible for the change.

Conclusion

The mixing ratio of SO_2 at the cloud top of Venus, derived from rocket observations made on 15 March 1988, and on 29 March 1991 is 80±40 and 120±60 ppb, respectively, and the scale height of SO_2 is 3±1 km. The mixing ratio of SO above the cloud derived from the 1991 observation is 10±5 ppb above the clouds. The scale height of SO is nearly the same as that of the bulk atmosphere, and the mixing ratio of SO decreases below the 64 km level. The derived mixing ratios and the scale height of SO_2 and SO are in good agreement with results from Pioneer Venus, IUE, and Venera-15 observations.

Acknowledgment

This research was supported the National Aeronautics and Space Administration under research grant NSG 5103.

REFERENCES

Barker, E.S., (1979): Detection of SO_2 in the UV spectrum of Venus, *Geophys. Res. Letters*, **6**, 117-120.

Clancy, R. T. and D. O. Muhleman (1991): Long term (1979-1990) changes in the Thermal, Dynamical, and Compositional Structure of the Venus atmosphere as inferred from Microwave Spectral line observations of ^{12}CO, ^{13}CO, and $C^{18}O$, *Icarus*, **81**, 129

Conway, R.R., McCoy, R.P., Barth, C.A. and Lane, A.L., (1979): IUE detection of SO_2 in the atmosphere of Venus, *Geophys. Res. Letters*, **6**, 629-631.

Del Genio, A. D. and W. B. Rossow (1989) Planetary-Scale Waves and the Cyclic Nature of Cloud Top Dynamics on Venus, *J. Atmos. Sci.*, **47**, 293-318.

Esposito, L.W., (1979): An "Adding" algorithm for the Markov chain formalism for radiation transfer, *Ap. J.*, **233**, 661-663.

Esposito, L.W., (1984): Sulfur Dioxide: Episodic injection shows evidence for active Venus volcanism, *Science*, **223**, 1072-1074.

Esposito, L.W. and House, L.L., (1978): Radiative transfer calculated from a Markov chain formalism, *Ap. J.*, **219**, 1058-1067.

Esposito, L.W., Copley, M., Eckert, R., Gates, L., Stewart, A.I.F. and Worden,H., (1988): Sulfur dioxide at the Venus cloud tops, 1978-1986, *J. Geophys. Res.*, **93**, 5267-5276.

Esposito, L.W., Winick, J.R. and Stewart, A.I.F., (1979): Sulfur dioxide in the Venus atmosphere: Distribution and implications, *Geophys. Res. Letters*, **6**, 601-604.

Freeman, D.E., Yoshino, K., Esmond, J.R., and Parkinson, W.H., (1984): High resolution absorption cross section measurements of SO_2 at 213 K in the wavelength region 172-240 nm, *Planet. Space Sci.*, **32**, 1125-1134.

Gurnett, D. A. et al. (1991), *Science*, **253**, 1522-1525

Head, J. W. (1991), *BAAS*, **23**, No. 3, 1205

Ksanfomaliti, L. W. (1980), *Nature*, **284**, 244

Kawabata, K., Hansen, J.E., (1975): Interpretation of the variation of polarization over the disk of Venus, *J. Atmos. Sci.*, **32**, 1133-1139.

McClintock, W.E. et al. (1982): Rocket-borne instrument with a high-resolution microchannel plate detector for planetary UV spectroscopy, *Applied Optics*, **21**, 3071-3079.

McClintock, W. E., C. A. Barth, R. A. Kohnert (1994): Sulfur Dioxide in the Atmosphere of Venus: Sounding Rocket Observations, *Icarus*, this issue.

Na, C.Y., Esposito, L.W. and Skinner, T.E., (1988): IUE observation of Venus SO_2, *Bulletin of American Astronomical Society*, **20**, No. 3, 832.

Na, C. Y., L. W. Esposito, and T. E. Skinner (1990): International Ultraviolet Explorer observation of Venus SO_2 and SO, *J. Geophys. Res.*, **95**, 7485.

Na, C. Y. (1992) Ph. D dissertation, U. of Colorado.

Owen T. and Sagan, C. (1972), Minor constituents in Planetary atmospheres: Ultraviolet Spectroscopy from the Orbiting Astronomical Observatory, *Icarus*, **16**, 557-568.

Phillips, L. F. (1981) Absolute Absorption Cross Sections for SO between 190 and 235 nm, J. Phys. Chem., **85**, 3994-4000.

Scarf F.L. et al. (1980): Lightning on Venus: Orbiter detection of whistler signals, *J. Geophys. Res.*, **85**, 8158-8166.

Shia, R.L., Y.L. Ha, J.S. Wen and Y.L. Yung (1990): Two dimensional atmospheric transport and chemistry model: Numerical experiments with a new advection algorithm. *J. Geophys. Res.*, **95**, 7467-7483.

Stewart, A.I.F., Anderson, D.E., Esposito, L.W. and Barth, C.A. (1979): Ultraviolet spectroscopy of Venus: Initial results from the Pioneer Venus Orbiter, *Science*, **203**, 777-778.

Taylor H. A. and Cloutier, P. A. (1986): Venus: Dead or Alive?, *Science*, **234**, 1087-1093.

VanHoosier M.E., Bartoe J.F., Brueckner, G.E. and Prinz, D.K., (1988): Absolute solar spectral irradiance 120nm - 400nm, *Astrophys. Lett. Commun.*, **27**, 163-168

Wilson, W.J., Klein, M.J., Kahar, R.K., Gulkis, S. and Olsen, E.T., (1981): Venus, 1. Carbon monoxide distribution and molecular-line searches, *Icarus*, **45**, 624-637.

Winick, J. R. and A. I. F. Stewart (1980) Photochemistry of SO2 in Venus' Upper Cloud Layers, *J. Geophys. Res.*, **85**, 7849-7860.

Yung, Y. L. and W. B. DeMore (1982) Photochemistry of the Stratosphere of Venus, *Icarus*, **51**, 199-247.

Zasova, L. V., V. I. Moroz, L. W. Esposito and C. Y. Na (1993): SO_2 in the middle atmosphere of Venus: IR measurements from Venera-15 and Comparison to UV data, *Icarus*, **105**, 92-109.

Table 1. Physcal parameters of Venus during Rocket observations

Rocket	27.110	36.078
Date	Sept 15, 1988	March 29, 1991
Elongation	Western	Eastern
Phase Angle	76.5°	51.6°
Angular size	18.8″	13.1″
Defect of Illumination	0.38	0.18
Slit size	1″ x 150″	2″ x 150″
Latitude Coverage	80°S - 40°N	10°S - 10°N

Table 2. Model parameters for Rocket observations

SO_2 mixing ratio	SO mixing ratio	SO_2 scale height
12.5 ppb	1.25 ppb	1 km
25	3.125	2
50	6.25	3
100	12.5	4
125	25	5
250	50	
500		
1000		

Figure Captions

Figure 1: Slit positions on the disk of Venus are shown for the rocket observations carried out in September 15, 1988 and March 29, 1991. Also shown are the points where model calculations were carried out.

Figure 2: SO_2 mixing ratios above the clouds of Venus derived from Pioneer Venus, IUE, Venera-15 and CU/LASP sounding rocket observations. These four different observations show a good agreement.

Figure 3: The 36.078 rocket spectrum is plotted with a model cotaining 100 ppb of SO_2 in the upper panel and a model containing 100 ppb of SO_2 and 12.5 ppb of SO in the lower panel. The model with SO give a much better fit to the data.

Figure 4: The vertical profile of SO derived from the 1991 observations is plotted with the predicted vertical profiles of SO from photochemical models by Winick and Stewart [1980] and Yung and DeMore [1982]

Figure 5: Mixing ratio and scale height of SO_2 derived from 1988 observation are plotted against latitude. The SO_2 mixing ratio at mid-latitude is much higher than at other latitudes, and the scale height of SO_2 shows an opposite trend.

Figure 6: Rocket reflectances at 2100 Å are shown in in solid lines. Dotted lines are model reflectances at 2100 Å that were calculated with different mixing ratios of SO_2 with the scale height fixed at 3 km. It is clear that the horizontal variation is not due to pointing errors.

Figure 7: SO_2 mixing ratios and scale heights derived from Venera-15 and the sounding rocket observations are plotted against latitude. The results are binned in 15° bins to reduce the scatter in the data.

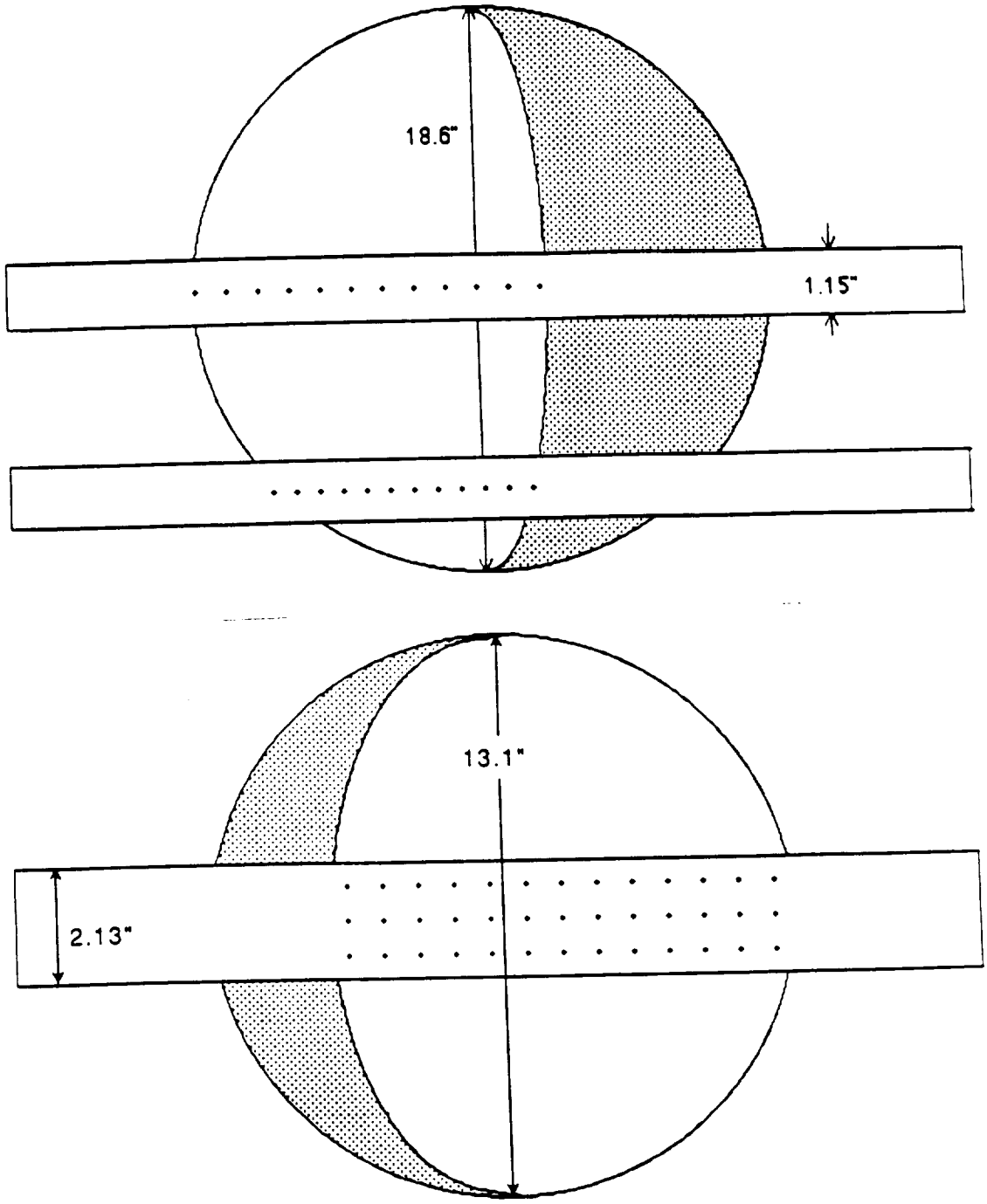

Figure 1: Slit positions on the disk of Venus are shown for the rocket observations carried out in September 15, 1988 and March 29, 1991. Also shown are the points where model calculations were carried out.

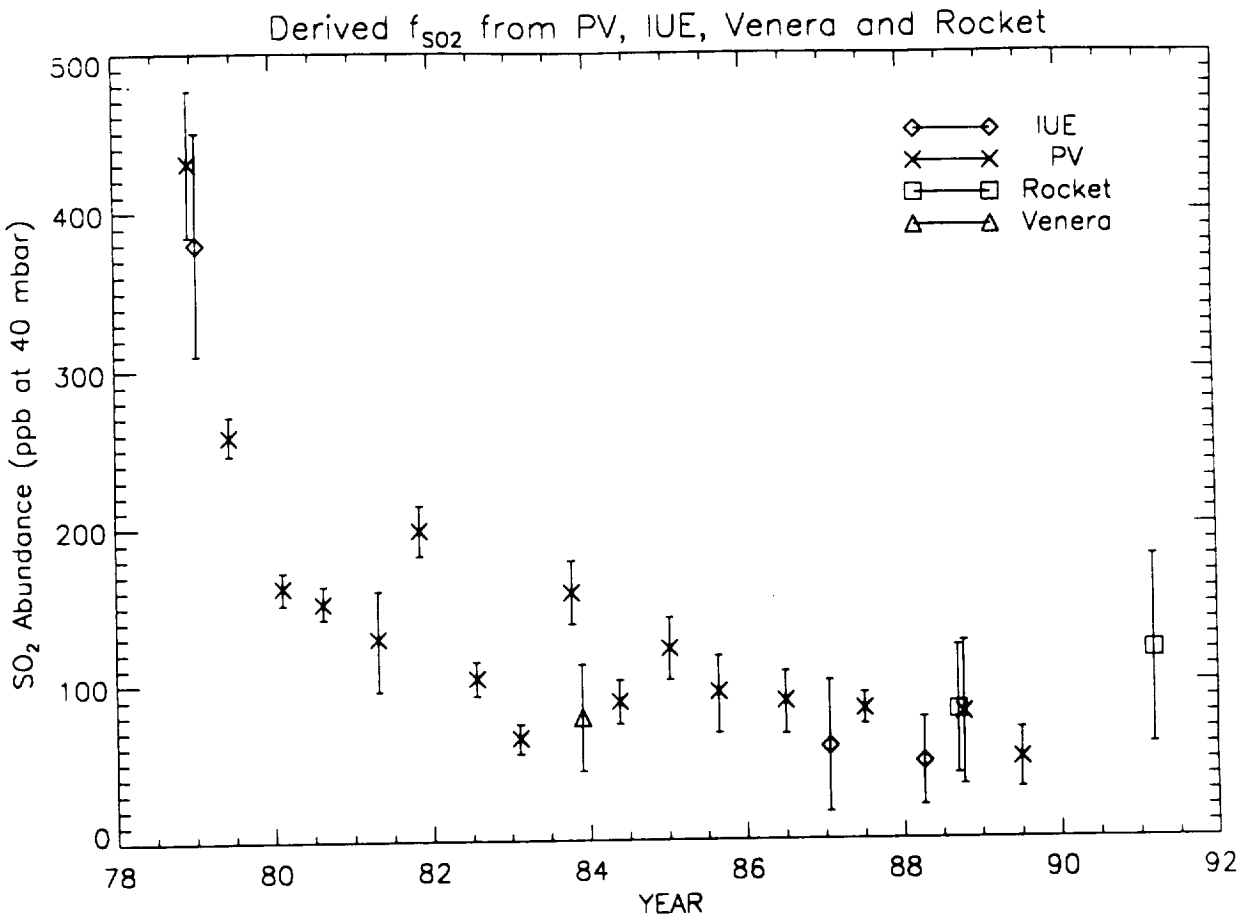

Figure 2: SO_2 mixing ratios derived from Pioneer Venus, IUE, Venera-15 and our sounding rocket observations. These four different observations show a good agreement.

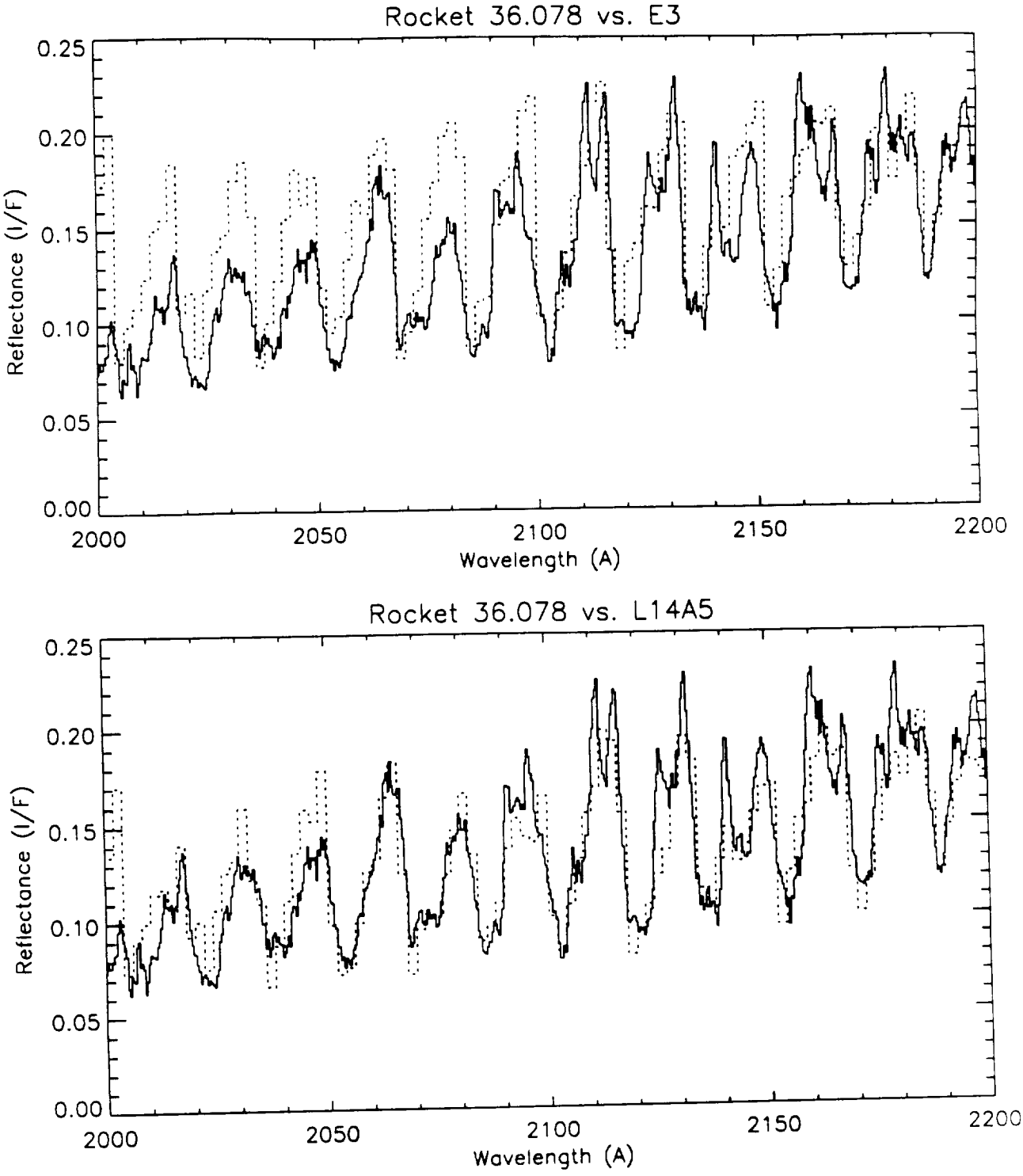

Figure 3: Rocket spectrum is plotted here with a model cotaining 100 ppb of SO_2 in the upper panel and a model containing 100 ppb of SO_2 and 12.5 ppb of SO in the lower panel. The model with SO fit the data much better.

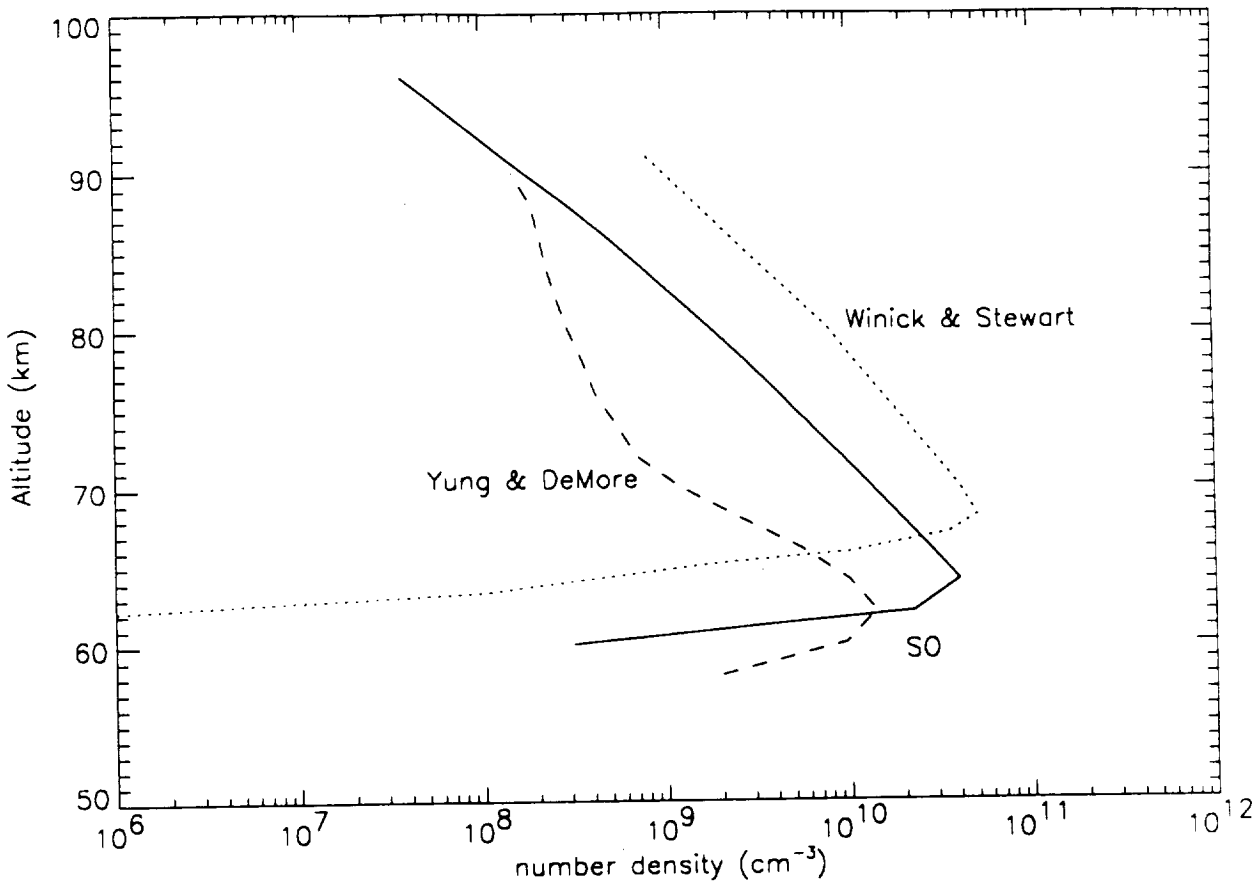

Figure 4: The vertical profile of SO derived from 1991 observations are plotted with the predicted vertical profiles of SO from photochemical models by Winick and Stewart [1980] and Yung and DeMore [1982]

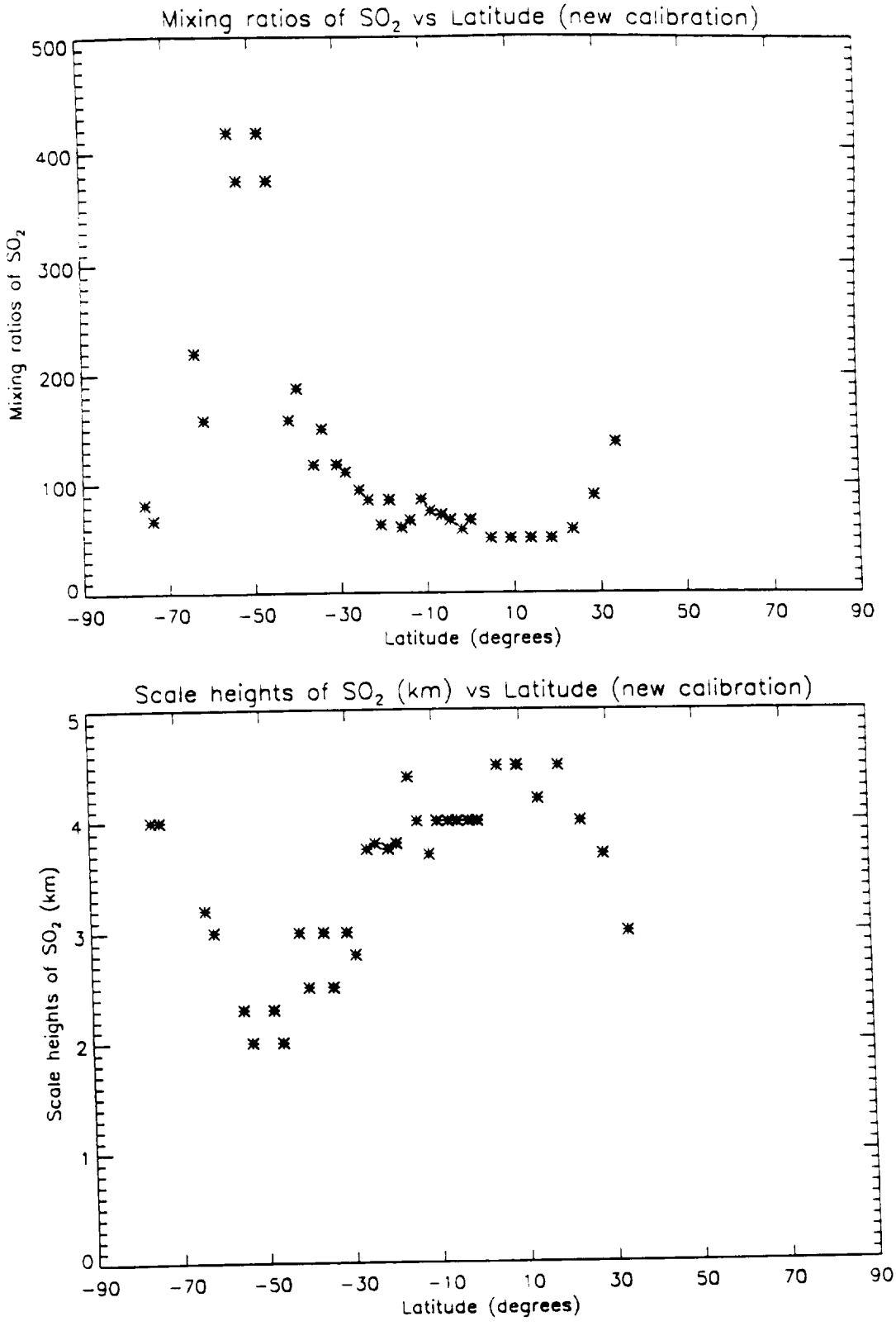

Figure 5: Mixing ratio and scale height of SO_2 derived from 1988 observation are plotted against latitude. The mixing ratio and scale height of SO_2 show anti-correlation.

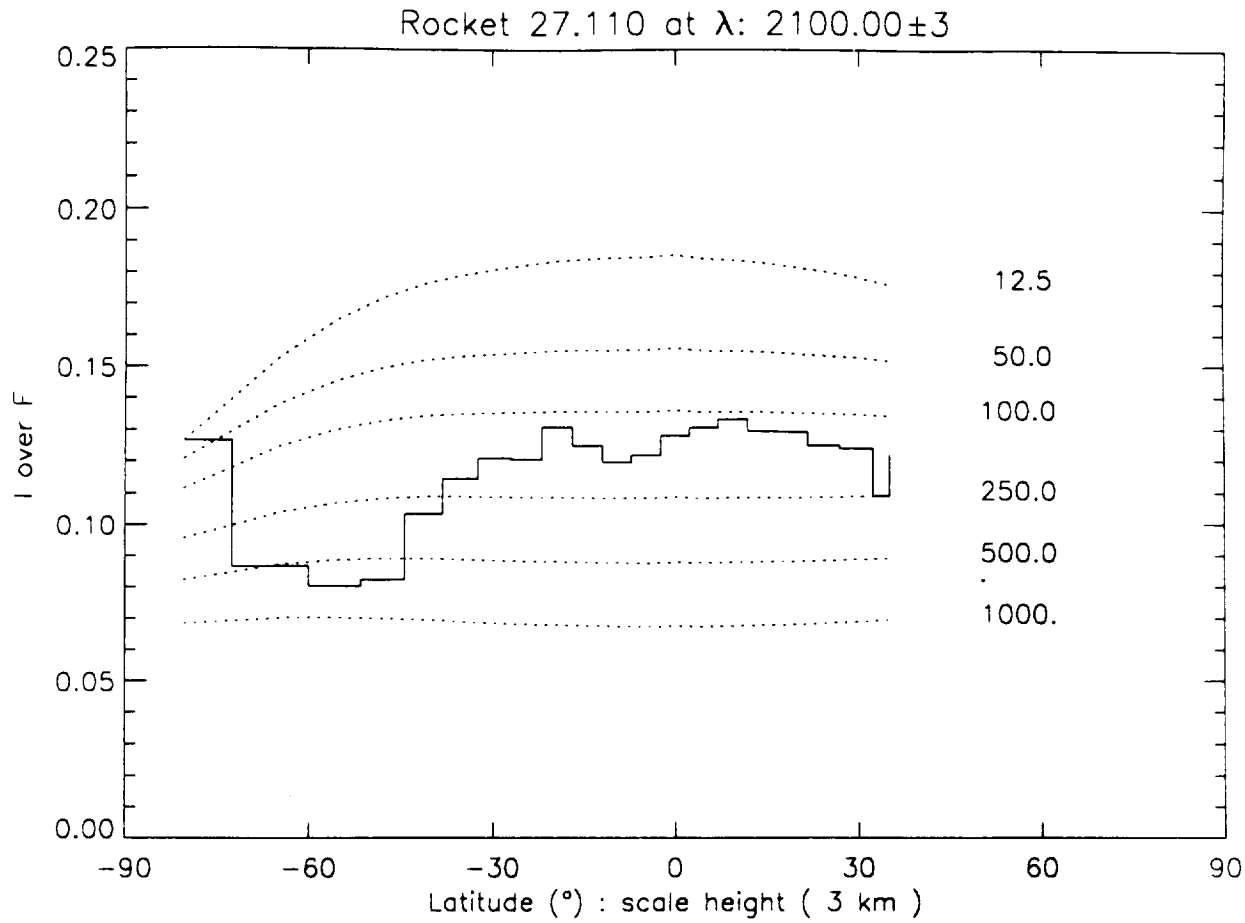

Figure 6: Rocket reflectances at 2100 Å are shown in in solid lines. Dotted lines are model reflectances at 2100 Å that were calculated with different mixing ratios of SO_2 while the scale height was fixed at 3 km. It is clear that the horizontal variation is not due to pointing errors.

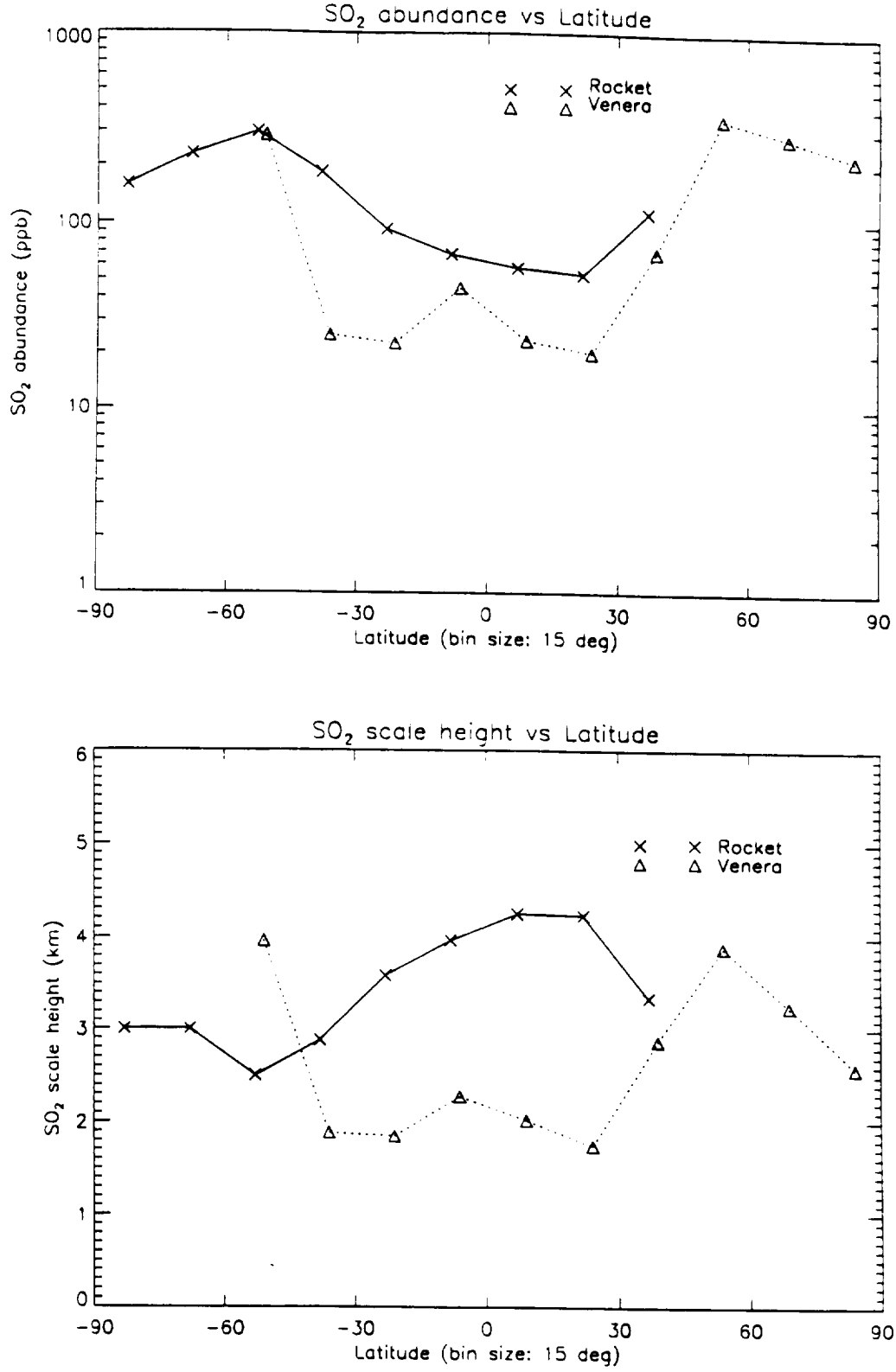

Figure 7: SO_2 mixing ratios and scale heights derived from Venera-15 and the sounding rocket observations are plotted against latitude. The results are binned in 15° bins to reduce the scatter in the data.